Thermal conductivity of superconducting alloy films in a perpendicular magnetic field*†

J. O. Willis‡ and D. M. Ginsberg
Department of Physics and Materials Research Laboratory, University of Illinois, Urbana, Illinois 61801
(Received 26 January 1976)

We have measured the thermal conductivity of superconducting films of indium-bismuth alloys in a perpendicular magnetic field. The films were condensed onto glass substrates held at 77 K, and had thicknesses ranging from 1050 to 4570 Å. Values of the ratio of the BCS coherence length to the electron mean free path for these films were $\simeq 9$. We made measurements at temperatures T between 0.3 and 1.0 K for magnetic fields ranging from zero to above the upper critical field H_{c2}. We plotted the thermal conductivity as a function of magnetic field. The resulting curve, except for some rounding very close to H_{c2}, was found to be approximately linear for magnetic fields greater than 60% of H_{c2}. This linear behavior is in qualitative agreement with the theory of Caroli and Cyrot for the electronic part of the thermal conductivity of a dirty superconductor near H_{c2}. This theory predicts that the ratio of the slope of the thermal-conductivity curve to the slope of the magnetization curve at H_{c2} is a universal function of the reduced temperature $t = T/T_c$, where T_c is the zero-field transition temperature. We infer the magnetization of our films with the help of theoretical calculations which are based on the critical-field values. The experimental values of the ratio of the slopes are 10–30% below the theoretical values. In attempting to explain this discrepancy, we speculate that κ_2 varies more rapidly as a function of temperature than theory predicts. The same conclusion has been drawn previously from both similar and different types of experiments.

I. INTRODUCTION

A type-II superconductor in a magnetic field H which is slightly less than the upper critical field H_{c2} exhibits the phenomenon of gapless superconductivity,[1] in which there is no energy gap in the electronic excitation spectrum. Gapless superconductivity was first predicted by Abrikosov and Gor'kov for a superconductor with dilute magnetic impurities.[2] Maki[3] and de Gennes[4] have shown that there is a formal correspondence between this system and a type-II superconductor just below H_{c2}, providing the ratio of the Bardeen-Cooper-Schrieffer[5] (BCS) coherence length to the transport electron mean free path is much greater that 1 ($\xi_0/l_{\rm tr} \gg 1$), which is called the "dirty" limit. In each case an external perturbation acts to break the Cooper pairs. We have measured the thermal conductivity of a superconductor in a magnetic field to test the validity of theoretical calculations of this transport property. We have chosen to measure the conductivity in thin films rather than bulk samples because bulk specimens usually have a large phonon thermal conductivity which is dependent on the magnetic field, making the determination of the electronic part of the thermal conductivity difficult. While there have been measurements of the thermal conductivity of bulk superconductors in the mixed state, that is, just below H_{c2}, there have apparently been no similar measurements on thin films which could be quantitatively compared to theory.

We have performed thermal-conductivity measurements on thin films of indium with approximately 2-at.% bismuth. We chose indium because it is a weak-coupling superconductor and does not oxidize rapidly; we chose bismuth for its reasonably large solubility in indium[6] and for its ability to cause both mass difference and valence scattering in indium. The alloys were condensed onto substrates held at 77 K. This procedure produces films with very short electron and phonon mean free paths. The short electron mean free path justifies the use of a diffusion equation for the electron motion, which is the basis for the dirty-limit theory of superconductors in a high magnetic field. The short phonon mean free path effectively quenches the phonon conductivity, and it does not have to be subtracted from the measured thermal conductivity to obtain the electronic component.[7,8] The thermal conductivity was measured as a function of the applied magnetic field, which was oriented perpendicular to the film.

II. THEORY

Ambegaokar and Griffin[9] have calculated the electronic part of the thermal conductivity of a dirty superconductor with magnetic impurities as a function of the pair-breaking interaction strength. Their result reduces to the Bardeen, Rickayzen, and Tewordt[10] (BRT) result when the pair breaking goes to zero. Ambegaokar and Griffin's result is based on a model in which the superconducting order parameter $\Delta(\vec{r})$ is independent of position; Caroli and Cyrot[11] have generalized this result to the case where $\Delta(\vec{r})$ varies with position. They find that to first order in the spatial average of the mean-square order parameter $\langle|\Delta|^2\rangle$, the conductivity is given by

$$K - K_n = -\frac{\sigma\langle|\Delta|^2\rangle}{2e^2T}\rho[\psi^{(1)}(\tfrac{1}{2}+\rho)+\rho\psi^{(2)}(\tfrac{1}{2}+\rho)], \quad (1)$$

where σ is the normal-state electrical conductivity, ρ is determined implicitly from the relation

$$\ln(T/T_c) = \psi(\tfrac{1}{2}) - \psi(\tfrac{1}{2}+\rho), \quad (2)$$

T_c is the transition temperature in the absence of pair breaking ($\rho = 0$), and $\psi^{(m)}(x)$ is the mth derivative of the digamma function $\psi(x)$.[12] Caroli and Cyrot attribute to Maki the calculation of this value of the mean-square order parameter:

$$\langle|\Delta|^2\rangle = -4\pi Mec k_B T/\sigma\psi^{(1)}(\tfrac{1}{2}+\rho) \quad (3)$$

for a type-II superconductor in a magnetic field near H_{c2}, where M is the magnetization, which is linear in magnetic field near H_{c2}. Substituting Eq. (3) into Eq. (1), taking the derivative of both sides with respect to the applied field H_a, evaluating the derivatives at H_{c2}, rearranging terms, and defining the function

$$U(t) = \left[\frac{dK}{dH_a}\Big/\left(4\pi\frac{dM}{dH_a}\right)\right]_{H_a=H_{c2}}, \quad (4)$$

we obtain Caroli and Cyrot's theoretical value of U,

$$U_{\rm th}(t) = \frac{ck_B}{2e}\rho\left(1+\frac{\rho\psi^{(2)}(\tfrac{1}{2}+\rho)}{\psi^{(1)}(\tfrac{1}{2}+\rho)}\right). \quad (5)$$

$U_{\rm th}$ depends only on the reduced temperature $t = T/T_c$ through Eq. (2).

In order to compare the theoretical result given in Eq. (5) with experiment, it is necessary to determine the slope of the magnetization curve at H_{c2}. To do this, we begin with the Abrikosov[13] expression for the magnetization of a bulk type-II superconductor as generalized by Maki[3] for all temperatures in the dirty limit,

$$4\pi\frac{dM}{dH} = \frac{1}{\beta[2\kappa_2^2(t)-1]}. \quad (6)$$

$\kappa_2(t)$ is the second generalized Ginzburg-Landau κ parameter and $\beta = \langle|\Delta|^4\rangle/\langle|\Delta|^2\rangle^2 \simeq 1.16$; we also use the relation $H_{c2} = \sqrt{2}\kappa_1(t)H_c(t)$, which defines $\kappa_1(t)$. For a thin film in a perpendicular magnetic field, the applied field H_a is not equal to the internal field H because of the large demagnetizing effects of the sample. Cape and Zimmerman[14] and Fetter and Hohenberg[15] find that the slope of the magnetization curve, as a function of applied magnetic field for a sample with demagnetizing factor n, is given by

$$4\pi\frac{dM}{dH_a} = \frac{4\pi\, dM/dH}{1+4\pi n\, dM/dH}. \quad (7)$$

For a thin circular film with radius R in a perpendicular field, $n \simeq 1 - (\frac{1}{2}\pi)d/R$,[16] where d is the film thickness; for a typical film $d/R \simeq 10^{-4}$, so that $n \simeq 1$. Using this result and Eqs. (6) and (7), we find the slope of the magnetization:

$$4\pi\frac{dM}{dH_a} = \frac{1}{\beta(2\kappa^2-1)+1}. \quad (8)$$

Lasher[17] performed detailed calculations of the properties of thin films in a perpendicular magnetic field near H_{c2}; his technique explicitly took into account the proper boundary condition for the magnetic field at the surfaces of the film. He calculated the free-energy density of the film, from which we find the magnetization near H_{c2} for $n = 1$,

$$4\pi\frac{dM}{dH_a} = \frac{1}{2\kappa^2 D(\kappa,d)}. \quad (9)$$

We generalize this result to all temperatures, following Maki,[3] by replacing κ with $\kappa_2(t)$. The value of the function $D(\kappa,d)$ depends on the arrangement of the vortices in the film; for the triangular vortex lattice with one flux quantum $\phi_0 = hc/2e$ per lattice site, which is the stable state for our films and for bulk type-II superconductors[18] ($\kappa > 1/\sqrt{2}$), D satisfies the equation

$$2\kappa^2 D = 2\kappa^2\beta - L(\eta), \quad (10)$$

where

$$L(\eta) = \sum_{m,n=-\infty}^{\infty}{}' e^{-I^2/2}\left(\frac{e^{-\eta I}-1+\eta I}{\eta I}\right), \quad (11)$$

$$I = [(4/\sqrt{3})\pi(m^2+mn+n^2)]^{1/2}, \quad (12)$$

where η is the ratio of the film thickness d to the coherence length $\xi = (\hbar c/2eH_{c2})^{1/2}$, and the prime in the sum over integers m and n indicates that the term in the sum $m = n = 0$ is to be omitted. The dependence of L on η is shown in Fig. 1. For $\eta \gg 1$, $L \simeq \beta - 1 \simeq 0.16$, so that Eq. (9) reduces approximately to Eq. (8). For $\eta \ll 1$, we find the

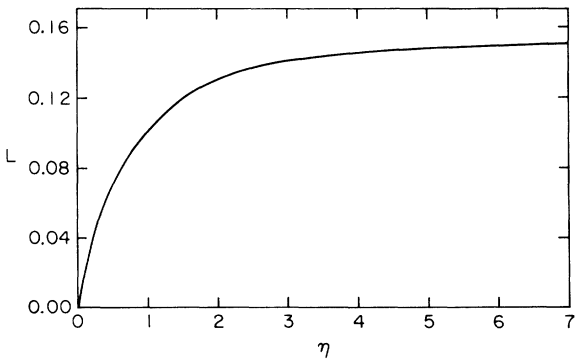

FIG. 1. L, the thickness-dependent term defined by Eq. (11), vs η, the ratio of the film thickness to the coherence length.

limiting behavior $L(\eta) \simeq 0.215\eta$. Nedellec *et al.*[19] also calculated $L(\eta)$ and obtained a coefficient of η which is smaller than our result by a factor $\frac{1}{4}\sqrt{3}$, for $\eta \ll 1$. They also calculated $L(\eta \ll 1)$ for the square vortex lattice and obtained a result for the coefficient of η which is smaller by a factor $\frac{1}{2}$ than the correct result of 0.230. D for the square lattice can be obtained from Eq. (12) by replacing I with $I_{sq} = [2\pi(m^2+n^2)]^{1/2}$ and by replacing β with $\beta_{sq} = 1.18$. We believe that Nedellec *et al.* somehow inverted the correct numerical coefficients in the expressions for I and I_{sq} in the product ηI of Eq. (11). Only our result agrees with Fig. 1 of Lasher's article.[17]

III. EXPERIMENT

A. Sample preparation

The alloy sample material was prepared by melting together the appropriate weights of 99.999%-pure indium and 99.999%-pure bismuth in an evacuated Pyrex tube, with the aid of an rf induction furnace. The alloy inside the tube was quenched in water from just above the melting point. The alloy ingot was then removed from the tube and mixed mechanically by folding and pressing it to insure homogeneity. Chemical analysis of the ingot gave a bismuth concentration of 1.99 ± 0.03 at.%. An impurity analysis revealed nothing which would affect the measurements or results.

Two samples were prepared for each run, one for the thermal-conductance measurement, and the other for the electrical-resistance measurement. The latter sample was used only to determine the resistive transition in zero magnetic field. The substrates for the thermal-conductance samples were number 00 Pyrex cover slides; they were 2.5 cm square and 0.0076 cm thick. Number 1 Pyrex cover slides were used for the electrical-resistance samples. The substrates were cleaned in detergent and hot water, then rinsed in deionized water, reagent-grade acetone, and reagent-grade isopropanol. The substrates were vapor degreased in freshly distilled isopropanol for several hours. Substrates which passed visual inspection were attached to a copper disk, with a drop of glycerine providing thermal contact. A mask was placed over the resistance-sample substrate to define a four-terminal resistor. Another mask covered a strip on each of two opposite sides of the thermal-conductance sample substrate.

The copper disk was then mounted in a glass bell jar for the condensation of the film. The disk was thermally grounded to a liquid-nitrogen container by means of screws and a thin layer of indium. A resistively-heated tungsten boat located 24 cm below the substrates was used to flash-evaporate 50 to 100 alloy pellets which had previously been placed on a Mylar conveyor belt. By turning a knob outside the bell jar, one could advance the conveyor belt to drop the pellets through a water-cooled chute into the boat. It was necessary to flash-evaporate the alloys because the vapor pressure of bismuth is much greater than that of indium at any given temperature; evaporation of a single large charge would have resulted in a layer of bismuth covered by a layer of indium on the substrate. A quartz-crystal thickness monitor was located near the substrates, and a moveable shutter was located 4 cm above the vapor source. Liquid-nitrogen traps in the roughing line and the high-vacuum line prevented back streaming of pump oil onto the substrates.

The bell jar was evacuated, and an auxillary liquid-nitrogen cold trap in the bell jar was filled. When the pressure had dropped to about 5×10^{-7} Torr, the container on which the substrates were mounted was filled with liquid nitrogen. Then the boat was heated and outgassed, the shutter was opened, and the conveyor belt was advanced to drop the pellets into the boat at the rate of about 1 pellet per sec. When the quartz-crystal monitor indicated that the film had reached the required thickness, the shutter was closed, and the boat power was turned off. The pressure remained below 10^{-6} Torr during the entire evaporation, which lasted about 1 min.

The bell jar was opened after the substrates had warmed to room temperature. The substrates were removed from the copper disk, and the glycerine was washed off with deionized water. The edges of the electrical-resistance sample were scribed to eliminate thin edges near the mask. The thermal-conductance sample was trimmed to a width of about 1.3 cm by scribing and breaking the glass along the edges that had been partially covered by the mask during the condensation of the sample. The two pieces of glass which were trimmed off were returned to the evaporator and cooled to 77 K, and a layer of pure indium about 1000 Å thick was condensed on the entire surface. The film thickness was then determined optically by multiple-beam interferometry[20] to an accuracy of ± 50 Å.

B. Low-temperature apparatus

The cryostat is shown in Fig. 2. It was designed to measure the thermal conductance and electrical resistance of thin-film samples in a plane perpendicular to an applied magnetic field. A ^{3}He refrigerator provided temperatures in the range 0.3–1 K. A superconducting solenoid provided a magnetic field up to 25 kOe. A paramagnetic salt

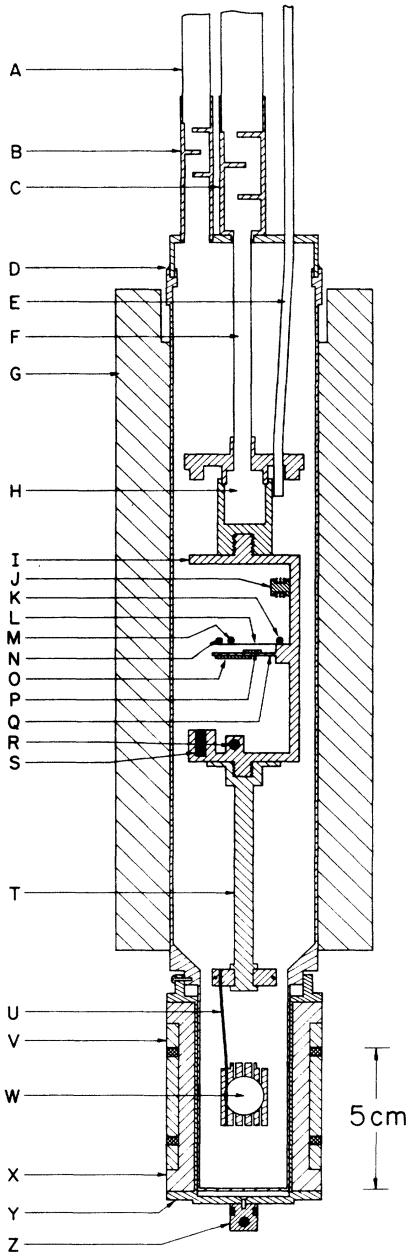

FIG. 2. Cross-section of the cryostat. A, cryostat pump-out line; B, light trap; C, light trap; D, Cd-Bi solder joint; E, electrical leads; F, ^{3}He pumping line; G, superconducting solenoid; H, ^{3}He tank; I, sample holder; J, electrical heating coil; K, carbon resistance regulating thermometer; L, thermal-conductance sample; M, carbon resistance measuring thermometer; N, sample heater; O, electrical-resistance sample; P, Hall probe; Q, copper sheet; R, germanium resistance thermometer; S, capacitance thermometer; T, copper link; U, copper wires (only one out of 17 is shown, for clarity); V, salt pill measuring secondary coil; W, salt pill; X, salt pill measuring primary coil; Y, coil form; Z, assembly of helium-bath carbon resistance thermometer and electrical heating coil.

pill (chrome methylamine alum) was the primary temperature standard below 1 K. A germanium thermometer, capacitance thermometer, and carbon-resistance thermometers were used as secondary thermometers. Bifilarly-wound manganin heaters were available for electronic temperature control. The T_{58} ^{4}He vapor-pressure scale was used to calibrate the thermometers, as described in greater detail elswhere.[21]

The capacitance thermometer was insensitive to magnetic fields,[22] and it was used as a null detector to determine the field dependence of the measuring thermometer M of Fig. 2 as follows. The capacitance of the capacitance thermometer was balanced on a bridge in zero field. The magnetic field was changed to a new value, the resistance of the carbon thermometer in the electronic regulator feedback loop was then adjusted until the capacitance bridge was balanced again, returning the temperature to its zero-field value. The changes in resistance of the carbon and germanium thermometers were then determined.

C. Magnetic field control and measurement

The superconducting solenoid was usually operated in the persistent mode. The field-to-current ratio of the solenoid was measured with a rotating-coil gaussmeter and with a nuclear-magnetic-resonance probe. The field variation was found to be smaller than 0.1% inside a 4-cm-diam sphere centered on the sample.

The strength of the magnetic field was determined from the solenoid current or from a Hall probe which was mounted 3 mm directly below the center of the thermal-conductance sample and in a plane parallel to the sample.

D. Method of measuring electrical resistance and thermal conductance

The electrical-resistance sample was thermally grounded to the bottom of copper sheet Q of Fig. 2 with a thin layer of Apiezon N grease. The current and voltage leads were attached to the sample with silver paint. The dc resistance of the sample was determined as a function of temperature in zero magnetic field.

The thermal conductance of the other sample plus the background conductance was measured with the aid of thermometers K and M and sample heater N, shown in Fig. 2. These three devices were Speer 470-Ω $\frac{1}{2}$-W carbon radio resistors which were ground flat on one side to facilitate mounting to the sample. Manganin leads, 10 cm long and 0.005 cm in diameter, were attached to the resistors with cadmium-bismuth solder; the conductance of the leads was approximately 1%

of the substrate conductance. Cadmium-bismuth solder was used to reduce the distortion of the magnetic field near the sample since this solder has a low superconducting transition temperature[23] and consequently a small critical field.[24] This solder was in the normal state for fields of interest in this experiment, which were on the order of a few hundred oersteds.

The bare side of the thermal-conductance sample was glued to the tab of the copper sample holder with GE 7031 varnish. The sample heater and carbon thermometers were glued with GE 7031 onto the film side of the sample to minimize thermal contact problems. No visible damage to the sample was caused by this technique. The regulating thermometer was glued to that part of the sample which was directly over the tab of the sample holder. The heater was mounted as close as possible to the other end of the sample. The measuring thermometer was located as close as possible to the heater without actually touching it. A common patch of glue connecting the heater and the measuring thermometer was avoided; it would have led to systematic errors in the values of the sample thermal conductivity.

The heater voltage was determined by the technique discussed by Neighbor[25] as follows. One-half of the power generated in the two equal-length manganin heater current leads was assumed to be dissipated in the sample holder and one-half in the heater. To take this into account, one heater voltage lead was connected to a current lead at the sample holder; the other voltage lead was connected to the remaining current lead at the heater. To correct for the thermoelectric effects, the current direction was reversed, and the product of the current and the average value of the voltage for the two current directions determined the heater power.

The measuring thermometer was calibrated against the germanium thermometer between 1.1 and 0.3 K in zero magnetic field for each data run. Typically 16 points were taken, and the rms deviation of the data from a four-parameter equation was about 0.5 mK.

The thermal conductance of each sample was measured at several temperatures between 1.0 and 0.3 K. At each temperature, the thermal conductance was measured for about 20 different magnetic field strengths. As the field was varied, the regulating thermometer, and therefore the cold end of the thermal-conductance sample, were kept at a fixed temperature by electronic feedback to the regulating heater J of Fig. 2. For each magnetic field value, the resistance R_{off} of the measuring thermometer, with the sample heater turned off, was measured. Then $\dot{Q}$, the power dissipated in the sample heater, was adjusted to produce the desired resistance value R_{on} of the measuring thermometer. The resistances R_{off} and R_{on} corresponded to temperatures T_{off} and T_{on} at the measuring thermometer. The temperature difference $\Delta T = T_{on} - T_{off}$ was about 10% of the average temperature of T_{off} and T_{on}. Approximately the same T_{off} and T_{on} were used for each value of the magnetic field. The heater power $\dot{Q}$ was then approximately proportional to the thermal conductance. The temperature calibration of the measuring thermometer was needed only to establish the absolute magnitude of the conductance and to correct for small differences in R_{off} and R_{on}; the relative values of the thermal conductances for different field strengths were therefore insensitive to possible small errors in the thermometer calibration.

Data were generally taken as the magnetic field was decreased in steps from the maximum value used. Data which were taken in increasing and decreasing fields gave the same results within experimental error at each field value. The magnetic field value measured near the sample with the Hall probe always agreed with the value calculated from the solenoid current to within experimental error. Both of these types of observations indicated a lack of flux trapping by the superconducting film. Flux trapping and associated hysteresis would have made the interpretation of the data very difficult.

Electrical power of less than 20 pW was dissipated in the regulating thermometer, and less than 3 pW was dissipated in the measuring thermometer. The heater power $\dot{Q}$ ranged from 3 to 100 nW. The temperature difference ΔT across the sample was measured to an accuracy of about $\pm 0.05\%$ at 1 K and of about $\pm 0.15\%$ at 0.4 K.

IV. RESULTS AND DISCUSSION

A. Electrical-resistance measurements

The transition temperature in zero magnetic field for the thermal-conductance sample was determined from the electrical-resistance sample. The results of these measurements are shown in Figs. 3 and 4. The transition temperature was defined as the temperature at which the electrical resistance of the sample attained one-half of its normal-state value. There is a small change in resistance of the samples at about 5.5 K. We believe that this behavior is due to a small amount of bismuth which precipitated out of the alloy during the cool down from 300 to 77 K. Resistive transitions are, of course, very sensitive to inhomogeneities, whereas thermal-conductivity measurements characterize the "bulk" of the

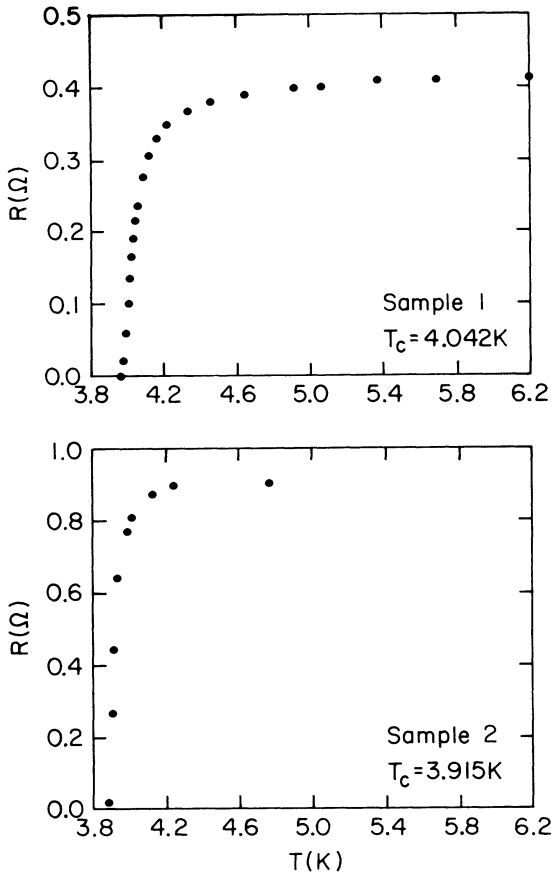

FIG. 3. Electrical resistance vs temperature in zero magnetic field for sample Nos. 1 and 2.

material. We have also made measurements on two samples, 2600 and 1600 Å thick, with a 4-at.% bismuth concentration[21]; we observed a change in resistance of about 25% of the normal-state value at 5.5 K. The resistivities for the 4-at.% samples

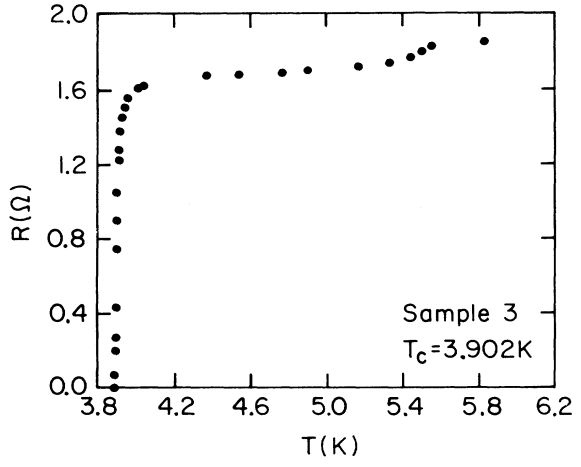

FIG. 4. Electrical resistance vs temperature in zero magnetic field for sample No. 3.

were within 15% of the values for the 2-at.% samples reported here. The final results for the ratio of the slope of the thermal-conductivity curve to the slope of the magnetization curve at H_{c2} for the 4-at.% Bi samples fall on the same line as the results for the 2-at.% samples.[21] This indicates that our results are not sensitive to inhomogeneities such as precipitates in the samples.

B. Thermal-conductance measurements

The only significant field-dependent contribution to the thermal conductance of the system of sample, substrate, and leads is the electronic part of the thermal conductance of the sample. The Pyrex substrate conductance is insensitive to magnetic fields of the magnitude used in this experiment.[26,27] The field dependence of the manganin leads should be small, and since the leads contribute only about 1% to the total conductance, their effect is negligible. The contribution of the sample's phonons to the thermal conductance is small also. Because of the lattice imperfections and small crystallite size resulting from the vacuum deposition of the film, the phonon mean free path is very short, greatly reducing the phonon conductance below the bulk value, and also below the value of the normal-state electronic part of the thermal conductance. This was shown by experiments performed above 1 K.[8] This situation should be even more favorable below 1 K; the phonon component vanishes as T^3, but the normal-state electronic component vanishes more slowly as T is decreased, since it is proportional to T. Any dependence of the substrate or lead conductance on field would create structure in the thermal-conductivity–versus–magnetic-field curve, and would appear at the same field value in each sample. Phonon field-dependent conductivity would result in a dip in the thermal-conductivity curve for small field values. We actually did observe small dips, but of less than 2% of the normal-state conductivity, in the data below 0.6 K for $H < 0.2H_{c2}$. These dips are at most 30% larger than the uncertainty in the data. Their presence probably indicates a small amount of background field dependence, which might have affected the calculated normal-state conductivity by 1 or 2%.

The first step in the data reduction was to obtain plots of thermal conductivity of the film alone, versus magnetic field. The equations used to calculate the conductivity $K(H)$ are

$$K(H) - K(0) = (L'/Wd)[KM(H) - KM(0)] \qquad (13)$$

and

$$K(0)/K(H) = (K_s/K_n)_{\mathrm{BRT}} \quad \text{for } H > H_{c2}, \qquad (14)$$

where

$$KM(H) = \dot{Q}(H)/\Delta T(H) \qquad (15)$$

is the total thermal conductance of the system in magnetic field H; $\dot{Q}(H)$ is the heater power dissipated to generate the temperature difference $\Delta T(H)$ in the sample; L', W, and d are, respectively, the sample length, width, and thickness; and $(K_s/K_n)_{BRT}$ is the BRT expression for the reduced thermal conductivity.[10] The value of $(K_s/K_n)_{BRT}$ was calculated using a value for the energy-gap width $2\omega_0(0) = 3.69 k_B T_c$.[28] $K(H)$ for $H > H_{c2}$ is the normal-state electronic thermal conductivity K_n. Below 0.7 K, the temperatures were corrected for the magnetic field dependence of the measuring thermometer. Above this temperature, the uncertainties in the correction were relatively large, and applying the correction would have tended to increase the scatter in the data. The correction above 0.7 K would have been only about 0.3% of the background conductance. The correction was therefore only made below 0.7 K. A correction was also made for the temperature dependence of the background conductance.[21] This correction was about 0.1% of the background conductance. This procedure slightly decreased the scatter in the data without introducing a systematic shift in them. Figures 5–7 show the reduced electronic thermal conductivity K/K_n as a function of applied magnetic field. The uncertainties shown represent ±1 standard deviation, and are almost entirely due to the uncertainties in determining the resistance of the measuring thermometer.

The reduced thermal conductivity does not depend on the geometry factor L'/Wd, but the normal-state conductivity does. The effective length L' of the sample is not as well defined as we would like, because of the finite widths of the thermometers and glue patches, so there may be significant uncertainties in the values of K_n. We have therefore chosen to calculate K_n by using the value of ρ which satisfies Eq. (2), since ρ is given by $\rho = D_0(H_{c2}e/2\pi c k_B T)$, where D_0 is the diffusion constant $v_F l_{tr}/3$, v_F is the Fermi velocity, and l_{tr} is the transport electron mean free path. K_n is given by $K_n = \gamma T D_0$, where $\gamma = 1079$ erg/cm^3 K^2 is the Sommerfeld specific-heat constant for pure indium.[29]

These values for K_n differ by less than 10% from those values calculated directly from the measured thermal conductances and geometry factors. We believe that the values of K_n calculated by using Eq. (2) are more accurate than those calculated by using the geometry factor, and we have therefore used the former values in the rest of the data analysis.

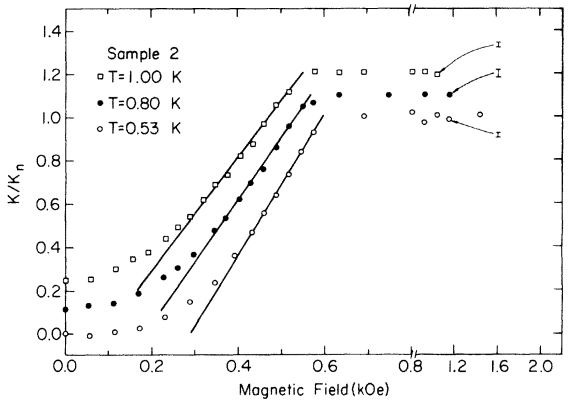

FIG. 6. Reduced thermal conductivity vs magnetic field for sample No. 2. The solid line determines the experimental slope. Data for $T = 0.80$ K and $T = 1.00$ K are shifted upward by 0.1 and 0.2, respectively, for clarity.

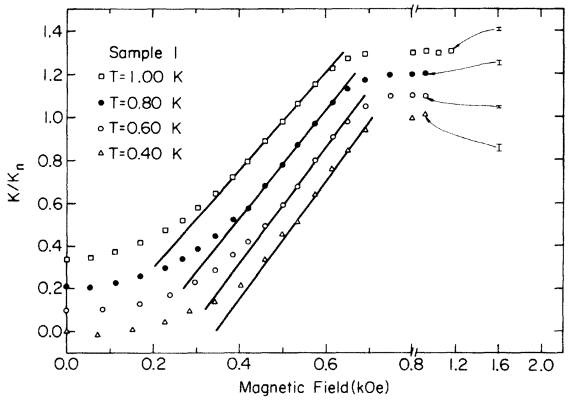

FIG. 5. Reduced thermal conductivity vs magnetic field for sample No. 1. The solid line determines the experimental slope. Data for $T = 0.60$ K, $T = 0.80$ K, and $T = 1.00$ K are shifted upward by 0.1, 0.2, and 0.3, respectively, for clarity.

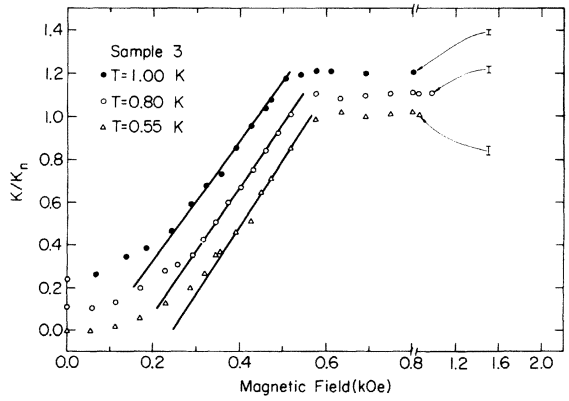

FIG. 7. Reduced thermal conductivity vs magnetic field for sample No. 3. The solid line determines the experimental slope. Data for $T = 0.80$ K and $T = 1.00$ K are shifted upward by 0.1 and 0.2, respectively, for clarity.

C. Slope of the reduced thermal conductivity at H_{c2}

A straight line was fitted by eye to the high-field region, where the data begin to drop from $K/K_n = 1.0$. The slope of this line was then defined to be the slope of the reduced thermal-conductivity curve at H_{c2}. These lines are shown in Figs. 5–7. The critical field H_{c2} was determined from the intersection of the straight-line fit to the reduced slope and the line $K/K_n = 1.0$. The uncertainties in determining H_{c2} include the uncertainty in determining the reduced slope and the uncertainty in the magnetic field measurements. Values of dK/dH_a at H_{c2} were determined as the product of the reduced slope and the normal-state conductivity which was calculated as described in Sec. IV B.

D. Slope of the magnetization curve at H_{c2}

We obtain the magnetization of the sample from the critical-field measurements and theoretical results. We calculate[3] $\kappa_1(T) = H_{c2}(T)/\sqrt{2}H_c(T)$, where we use the parabolic temperature dependence for H_c, $H_c(t) = H_c(0)(1-t^2)$, and $H_c(0)$ is the thermodynamic critical field at zero temperature. We scale $H_c(0)$ according to $H_c(0) = H_{cb}(0)T_c/T_{cb}$, where $H_{cb}(0) = 282.7$ Oe is the critical field, and $T_{cb} = 3.407$ K is the critical temperature for pure bulk indium.[29] T_c is the measured critical temperature for the sample, and T is the average temperature in the thermal-conductance measurement.

We determine $\kappa_2(T)$ from $\kappa_1(T)$ and the theoretical calculations of Eilenberger.[30] He calculated $\kappa_1(t)/\kappa$ and $\kappa_2(t)/\kappa$ as a function of t for several values of the parameters ξ'/l_{tr} and l_{tr}/l. He defined ξ' to be $\hbar v_F/2\pi k_B T_c$, so that $\xi' \simeq 0.883\xi_0$, where ξ_0 is the BCS coherence length; l_{tr} is the transport mean free path and l is the s-wave mean free path. ξ_0 is scaled according to[31] $\xi_0 = \xi_{0b}T_{cb}/T_c$ with $\xi_{0b} = 2460$ Å. l_{tr} is determined from the diffusion constant D_0, and $v_F = 0.61 \times 10^8$ cm/sec is the renormalized Fermi velocity.[31] The values of ξ_0/l_{tr} range from 8.7 to 10.0 for these films. There is no way to calculate l_{tr}/l for our films; Eilenberger suggests that the most likely value is $l_{tr}/l = 1.5$, which we have used in our calculations. We note that Eilenberger's calculations apply to bulk type-II superconductors, and we are applying them to films. There are no similar calculations of κ_1/κ and κ_2/κ for films, and the finite thickness might be expected to modify the results.

We calculate the slope of the magnetization curve at H_{c2} from κ_2, H_{c2}, the film thickness d, and Eq. (9). Important experimental quantities are listed in Table I.

E. Calculation of U_{expt}

The experimental values U_{expt} for U, which is defined in Eq. (4), are calculated from the results described in Secs. IV C and IV D. All derivatives are evaluated at H_{c2}. These values of U_{expt} are plotted in Fig. 8, along with the theoretical curve U_{th} of Eq. (5). The experimental uncertainties in the determination of U_{expt}, which are shown as vertical bars in Fig. 8, include the uncertainties in H_{c2}, K_n, T_c, and the K/K_n data, and the uncertainty in determining the reduced slope from the K/K_n data. The uncertainties in U_{expt} correspond to a standard deviation of about ±5%. We have not included any uncertainty from our choice of $l_{tr}/l = 1.5$ since we do not know the actual value of l_{tr}/l. We do, however, find that $U_{expt}(l_{tr}/l = 1.0)$ is 4–5% higher, and $U_{expt}(l_{tr}/l = 2.0)$ is 2–3% lower than $U_{expt}(l_{tr}/l = 1.5)$. This range of l_{tr}/l is expected to include any reasonable scattering potential, according to Eilenberger. We have also calculated

$$U_{cz} = \frac{dK}{dH_a}\{1.16[2\kappa_2^2(T) - 1] + 1\}, \tag{16}$$

which uses Cape and Zimmerman's approximate

TABLE I. Characteristics of the samples.

Sample	d (Å)	T/T_c	K_n (cgs)	l_{tr} (Å)	$\frac{dK}{dH_a}$ at H_{c2} (cgs)	H_{c2} (Oe)	κ_2
1	4570±40	0.099	18 280±280	208±3	50.2±2.0	711±3	1.562
		0.149	27 540±210	209±2	74.5±3.4	692±4	1.535
		0.198	36 820±430	210±3	92.8±2.5	668±5	1.504
		0.247	46 010±370	210±3	104.8±3.3	643±4	1.481
2	1970±30	0.134	27 130±300	235±3	87.5±3.1	600±3	1.378
		0.204	41 520±540	237±3	118.4±2.6	571±4	1.337
		0.256	51 660±640	235±3	134.5±4.9	551±4	1.332
3	1050±30	0.141	29 910±650	248±5	93.8±3.6	566±3	1.301
		0.205	43 220±690	246±4	127.5±3.0	547±3	1.282
		0.256	55 030±700	251±3	152.3±7.4	515±4	1.236

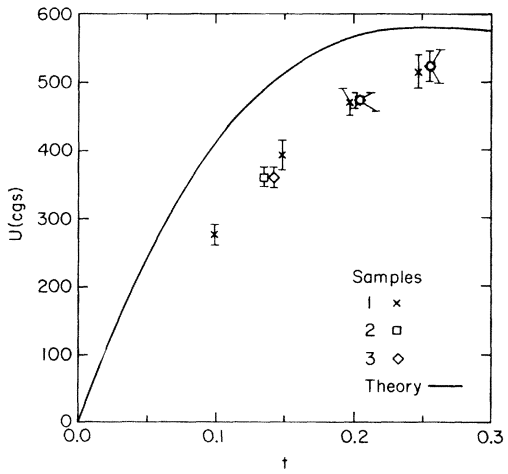

FIG. 8. Experimental values of U, defined in Eq. (4), and the theoretical curve, vs the reduced temperature.

expression for the magnetization instead of Eq. (9). Corresponding values of U_{expt} and U_{cz} differ by less than 1% for our films.

F. Discussion

Figures 5–7 show the data to be in excellent agreement with the linear dependence of the thermal conductivity on magnetic field near H_{c2}, which was predicted by Caroli and Cyrot.[11] However, there is a small amount of rounding very close to H_{c2}. The temperature difference $\Delta T \simeq 0.1T$ along the sample gives rise to a distribution of $H_{c2}(T)$ values along the sample, and these tend to smear out the transition. Other causes for the rounding could be variations in the film thickness or composition, resulting in variations in H_{c2}. The linear region extends down to fields of magnitude $H \simeq 0.6H_{c2}$.

The quantitative agreement with the theory of Caroli and Cyrot is only fair, however, as shown in Fig. 8. The experimental values of U are about 10% low near $t = 0.25$ and 30% low at $t = 0.10$. The experimental points lie nearly on a smooth curve for values of $\eta = d/\xi(t)$ ranging from 1.3 to 6.7 and for values of ξ_0/l_{tr} from 8.7 to 10.0. The curve which could be drawn through the experimental points has the same general shape as the theoretical curve.

We have considered three possible reasons for the observed deviation of the experimental results from the universal curve U_{th}. The first is that our samples, which have values of ξ_0/l_{tr} which are about 8.7–10.0, are not strictly in the dirty limit, $\xi_0/l_{tr} \gg 1$, which is assumed by Caroli and Cyrot. Thermal-conductivity measurements by Gupta *et al.*[32] on bulk type-II superconductors with $\xi_0/l_{tr} \simeq 10$–20 indicated values of U which were in good agreement with the theory. Muto *et al.*[33] obtained good agreement with theory for $0.4 < t < 0.8$ using alloys of $\xi_0/l_{tr} \simeq 5$–10. Del Vecchio and Lindenfeld[34] found results which are in good agreement with the theory for $\xi_0/l_{tr} > 16$ and $t > 0.4$. Below this reduced temperature, the experimental points were lower than the theoretical ones.

The experimental situation is not completely clear, particularly in light of the need to use questionable methods to account for the phonon contribution to the thermal conductivity in a magnetic field for those experiments on bulk samples. However, it seems reasonable to assume that values of $\xi_0/l_{tr} \geq 10$ are sufficient to obtain a limiting behavior for U.

A second possible interpretation of the discrepancy is that the theory of Caroli and Cyrot for the thermal conductivity is not correct, even when $\xi_0/l_{tr} \gg 1$. There is no clear evidence for this point of view, except possibly at low reduced temperatures.[34] Measurements of the thermal conductivity of thick films in the surface-sheath region by Smith and Ginsberg[26] agree with the calculations of Caroli and Cyrot and of Maki.[35] The expression for $\langle|\Delta|^2\rangle$ is different for this case, but the expression for the thermal conductivity as a function of $\langle|\Delta|^2\rangle$ is the same. Those measurements were made on tin films with $\xi_0/l_{tr} \simeq 2$–6 in the reduced temperature range $t < 0.3$. Tunneling measurements by Nedellec *et al.*[19] on indium-bismuth films with $\xi_0/l_{tr} \simeq 5$ and $t > 0.4$ in a perpendicular magnetic field showed good agreement with theoretical predictions. The tunneling characteristics depend on the same $\langle|\Delta|^2\rangle$ as do our measurements, verifying the correct theoretical expression for $\langle|\Delta|^2\rangle$.

The third possibility is that the discrepancy between our results and the theoretical prediction can be ascribed to the temperature variation of κ_2. If we assume that Eq. (5), the Caroli and Cyrot result, is correct, then our data can be used to calculate the values of κ_2. In Fig. 9 the values of $\kappa_2(t)/\kappa_2(1)$ determined from this calculation are shown as a function of t, with the Eilenberger result for $\kappa_2(t)/\kappa_2(1)$ with $\xi_0/l_{tr} = 9.3$ and $l_{tr}/l = 1.5$. The experimental points imply a much more rapid increase with decreasing t than Eilenberger's calculations indicate.

The experimental evidence concerning the κ_2 temperature dependence is somewhat inconsistent. Guyon[36] could explain his tunneling data with a more rapid variation with temperature of κ_2 than the theoretical prediction. However, his analysis of his measurements on indium alloys is in error,[19] and his corrected results may not show this discrepancy with theory. Magnetization measure-

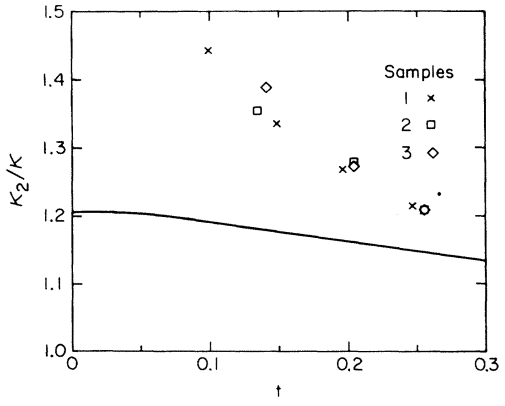

FIG. 9. $\kappa_2(t)/\kappa$ which would bring the experimental values of U, defined in Eq. (4), into agreement with the theoretical values. The solid line shows the results of Eilenberger's calculation for $\kappa_2(t)/\kappa$ with $\xi_0/l_{tr}=9.3$ and $l_{tr}/l=1.5$.

ments on indium-thallium and other alloys by Fischer and Vieli[37] are in good agreement with Eilenberger's predictions. Nedellec *et al.*[19] found a temperature variation of κ_2 which is about 5% faster than Eilenberger's calculation for the range $t>0.4$.

Magnetization measurements by Farrell *et al.*[38] on lead-indium alloys and by Fietz and Webb[39] on niobium-titanium alloys show large low-temperature values of κ_2/κ, compared with the theoretical results of Eilenberger. For $\xi_0/l_{tr}\simeq 9$ the result for lead-indium was $\kappa_2(0.2)/\kappa_2(1)\simeq 1.4$, and for niobium-titanium the result was $\kappa_2(0.1)/\kappa_2(1)\simeq 1.45$. It should be noted that lead is a strong-coupling superconductor, and its properties are frequently affected by this.[40,41] However, if this qualification for lead is not important, then the temperature variation of κ_2 in these two experiments is consistent with the variation of κ_2 which would bring our experimental results into agreement with theory.

We believe that the most likely reason for the discrepancy between our measurements of U and the theoretical prediction for it is a more rapid variation of κ_2 with temperature than the theoretical prediction of Eilenberger.[30]

G. Summary

We have measured the thermal conductivity of several superconducting indium-bismuth films with thicknesses ranging from 1000 to 4600 Å, and with $\xi_0/l_{tr}\simeq 9$, in a perpendicular magnetic field. The measurements were made for reduced temperatures $t<0.3$.

We compared our results to the theory of Caroli and Cyrot for the electronic thermal conductivity of a dirty superconductor near H_{c2}. Except for some rounding very close to H_{c2}, the measured thermal-conductivity curves exhibit the predicted linear dependence on magnetic field down to about $H=0.6H_{c2}$. The theory predicts that the ratio of the slope of the thermal-conductivity curve to the slope of the magnetization curve at H_{c2} is a universal function of the reduced temperature. We calculated the magnetization with the help of theoretical expressions which are based on critical-field values. The experimental values of the ratio of the slopes lie 10–30% below the theoretical values. We have discussed several hypotheses in an attempt to explain this discrepancy. We feel that the most plausible explanation is that κ_2 for our films varies more rapidly with temperature than the theoretical calculations of Eilenberger predict for bulk samples.

Other experiments on films and bulk samples have also yielded evidence for a more rapid temperature variation of κ_2 than the theory predicts. If the κ_2 parameters of our films have a temperature dependence similar to that observed in those other experiments, then our experimental results would be consistent with the theory of Caroli and Cyrot.

---

*Research supported in part by the National Science Foundation under Grant Nos. DMR-72-03026 and DMR-73-07581.

†Paper based in part on the Ph.D. thesis of J. O. Willis, University of Illinois, 1976.

‡Present address: Naval Research Laboratory, Washington, D.C. 20375.

[1]K. Maki, in *Superconductivity*, edited by R. D. Parks (Dekker, New York, 1969), Vol. 2, p. 1035.

[2]A. A. Abrikosov and L. P. Gor'kov, Zh. Eksp. Teor. Fiz. 39, 1781 (1960) [Sov. Phys.-JETP 12, 1243 (1961)].

[3]K. Maki, Physics 1, 21 (1964).

[4]P. G. de Gennes, Phys. Kondens. Mater. 3, 79 (1964).

[5]J. Bardeen, L. N. Cooper, and J. R. Schrieffer, Phys. Rev. 108, 1175 (1957).

[6]M. Hansen, *Constitution of Binary Alloys*, 2nd ed. (McGraw-Hill, New York, 1958), p. 313.

[7]D. E. Morris and M. Tinkham, Phys. Rev. 134, A1154 (1964).

[8]R. D. Parks, F. C. Zumsteg, and J. M. Mochel, Phys. Rev. Lett. 18, 47 (1967).

[9]V. Ambegaokar and A. Griffin, Phys. Rev. 137, A1151 (1965).

[10]J. Bardeen, G. Rickayzen, and L. Tewordt, Phys. Rev. 113, 982 (1959).

[11]C. Caroli and M. Cyrot, Phys. Kondens. Mater. 4, 285 (1965).

[12]H. T. Davis, *Tables of the Mathematical Functions* (Principia, San Antonio, 1935), Vol. I, p. 285.

[13]A. A. Abrikosov, Zh. Eksp. Teor. Fiz. 32, 1442 (1957)

[Sov. Phys.-JETP 5, 1174 (1957)].
[14]J. A. Cape and J. M. Zimmerman, Phys. Rev. 153, 416 (1967).
[15]A. L. Fetter and P. C. Hohenberg, Phys. Rev. 159, 330 (1967).
[16]L. D. Landau and E. M. Lifshitz, *Electrodynamics of Continuous Media* (Pergamon, London, 1960).
[17]G. Lasher, Phys. Rev. 154, 345 (1967).
[18]W. H. Kleiner, L. M. Roth, and S. H. Autler, Phys. Rev. 133, A1226 (1964).
[19]P. Nedellec, E. Guyon, and F. Brochard, J. Low Temp. Phys. 1, 519 (1969).
[20]S. Tolansky, *Multiple-Beam Interferometry of Surfaces and Films* (Oxford U. P., London, 1949).
[21]J. O. Willis, Ph.D. thesis (University of Illinois, Urbana, 1976) (unpublished).
[22]W. N. Lawless, in *Temperature, Its Measurement and Control in Science and Industry,* edited by H. H. Plumb (Instrument Society of America, Pittsburgh, 1972), Vol. 4, Part 2, p. 1143.
[23]J. F. Cochran, D. E. Mapother, and R. E. Mould, Phys. Rev. 103, 1657 (1956).
[24]H. W. Lewis, Phys. Rev. 101, 939 (1956).
[25]J. E. Neighbor, Rev. Sci. Instrum. 37, 497 (1966).
[26]J. E. Smith, Jr., and D. M. Ginsberg, Phys. Rev. 167, 345 (1968).
[27]R. A. Fisher, G. E. Brodale, E. W. Hornung, and W. F. Giauque, Rev. Sci. Instrum. 39, 108 (1968).
[28]J. M. Rowell, W. L. McMillan, and R. C. Dynes, J. Phys. Chem. Ref. Data (to be published).
[29]D. K. Finnemore and D. E. Mapother, Phys. Rev. 140, A507 (1965).
[30]G. Eilenberger, Phys. Rev. 153, 584 (1967).
[31]J. Feder and D. S. McLachlan, Phys. Rev. 177, 763 (1969).
[32]A. Gupta, S. Wolf, and B. S. Chandrasekhar, Solid State Commun. 10, 57 (1972).
[33]Y. Muto, K. Noto, T. Mamiya, and T. Fukuroi, J. Phys. Soc. Jpn. 24, 992 (1968).
[34]L. V. Del Vecchio and P. Lindenfeld, Phys. Rev. B 1, 1097 (1970).
[35]K. Maki, Phys. Rev. 148, 370 (1966).
[36]E. Guyon, Adv. Phys. 15, 417 (1966).
[37]E. Fischer and H. P. Vieli, Phys. Lett. A 26, 35 (1967).
[38]D. E. Farrell, B. S. Chandrasekhar, and H. V. Culbert, Phys. Rev. 177, 694 (1969).
[39]W. A. Fietz and W. W. Webb, Phys. Rev. 161, 423 (1967).
[40]D. J. Scalapino, in *Superconductivity,* edited by R. D. Parks (Dekker, New York, 1969), Vol. 1, p. 449.
[41]N. F. Masharov, Fiz. Tverd. Tela 16, 2342 (1974) [Sov. Phys.-Solid State 16, 1524 (1975)], and references listed therein.